

1           **Efficiency of the Summer Monsoon in Generating Streamflow within a**  
2           **Seasonally Snow-Dominated Headwater Basin of the Colorado River**  
3  
4

5           **Rosemary W.H. Carroll<sup>1,4</sup>, David Gochis<sup>2</sup>, and Kenneth H. Williams<sup>3,4</sup>**

6           <sup>1</sup>Desert Research Institute, Reno, NV, <sup>2</sup>National Center for Atmospheric Research, Boulder, CO,  
7           <sup>3</sup>Lawrence Berkeley National Laboratory, Berkeley, CA, <sup>4</sup>Rocky Mountain Biological Lab,  
8           Gothic, CO  
9

10          Corresponding author: Rosemary W.H. Carroll ([rosemary.carroll@dri.edu](mailto:rosemary.carroll@dri.edu))  
11

12          **Key Points:**

- 13           • Monsoons generate 10±6% of annual streamflow while late spring snowfall delivers  
14           twice as much for the same water input.
- 15           • The influence of monsoons on streamflow is lessened by evapotranspiration in the lower  
16           subalpine forest.
- 17           • Monsoon efficiency in generating streamflow decreases in years with low snow  
18           accumulation and high aridity.
- 19  
20

## 21 **Abstract**

22 The North American Monsoon occurs July-September bringing significant rainfall to  
23 Colorado River headwater basins. This rain may buffer streamflow deficiencies caused by  
24 reductions in snow accumulation. Using a data-modeling framework, we explore the importance  
25 of monsoon rain in streamflow generation over historic conditions in an alpine basin. Annually,  
26 monsoon rain contributes  $18\pm 7\%$  water inputs, generates  $10\pm 6\%$  streamflow and increases water  
27 yield  $3\pm 2\%$  the following year. The bulk of rain supports evapotranspiration in lower subalpine  
28 forests. However, rains have the potential to produce appreciable streamflow at higher elevations  
29 where soil storage, forest cover and aridity are low; and rebounds late season streamflow  
30  $64\pm 13\%$  from simulated reductions in snowpack as a function of monsoon strength. Interannual  
31 variability in monsoon efficiency to generate streamflow declines with low snowpack and high  
32 aridity, implying the ability of monsoons to replenish streamflow in a warmer future with less  
33 snow accumulation will diminish.

34

## 35 **Plain Language Summary**

36 Monsoon rains bring much needed summer moisture to the southwestern United States,  
37 but it remains unclear whether rains have a significant effect on streamflow in the snow-  
38 dominated headwaters of the Colorado River. Lack of understanding is largely due to the  
39 difficulty in measuring rain and snowfall in steep, mountainous basins, and the effect both have  
40 on seasonal plant consumption of water. Using a hydrological model populated with ground,  
41 airborne and synthesized climate data, we compare relative efficiency of monsoon rain to  
42 generate stream water over multiple decades. Monsoon rains deliver one-fifth of the basin's  
43 water and produce 10% the annual streamflow, with additions largely confined to the upper  
44 elevations of the watershed where soils are thin, water is plentiful, and forests are less abundant.  
45 In contrast, lower elevations contain dense aspen and conifer forests that consume monsoon rain  
46 and limit streamflow response. Subsequently, even strong monsoon events cannot fully replenish  
47 lost snow. Summer rains produce more streamflow during cooler years with large snow  
48 accumulation. This hints that streamflow from summer rain may diminish in a warmer future  
49 with less snow.

## 50 **1 Introduction**

51 Snowpack in mountain systems is declining worldwide with trends in snow loss expected  
52 into the future (Hock et al., 2019). Across the western United States (US), rising temperatures  
53 and changing precipitation patterns have decreased peak snow accumulation 15-30% since the  
54 mid-20<sup>th</sup> century (Mote et al., 2018), with the intensity and duration of these seasonal snow  
55 deficits increasing over the last 40 years (Huning & AghaKouchak, 2020). Reductions in snow  
56 cover produce a positive albedo feedback that results in higher air temperatures that promotes  
57 additional snowmelt (Hall, 2004; Ma et al., 2019). Rising temperatures can also drive larger soil  
58 evaporation and plant transpiration (evapotranspiration, ET) to reduce streamflow (Milly &  
59 Dunne, 2020). The Colorado River in the southwest US is dependent on 90% of its flow from the  
60 snow covered headwaters of Utah, Colorado and Wyoming (Jacobs, 2011) and is emblematic of  
61 these cascading feedbacks with 20% streamflow reductions projected by mid-21<sup>st</sup> century (Vano  
62 et al., 2012). The North American Monsoon (NAM) can bring significant rain to the region July  
63 to September (Sheppard et al., 2002) that has the potential to buffer streamflow deficiencies  
64 related to reductions in snowpack. Or the corollary, a lack of monsoon rain could potentially

65 promote late summer streamflow depletions and the potential to influence soil moisture memory  
66 on streamflow generation in the subsequent water year. To date, the influence of monsoon  
67 rainfall on streamflow generation in high elevation, snow-dominated basins remains uncertain  
68 largely due to difficulty in predicting and quantifying precipitation and snowmelt across  
69 mountainous watersheds (Deems et al., 2006; Harpold et al., 2012) and the tight coupling of  
70 climate, vegetation and topography ( Bales et al., 2006; Tennant, 2016; Tennant et al., 2017) that  
71 controls hydrologic partitioning between ET and runoff (Carroll et al., 2019).

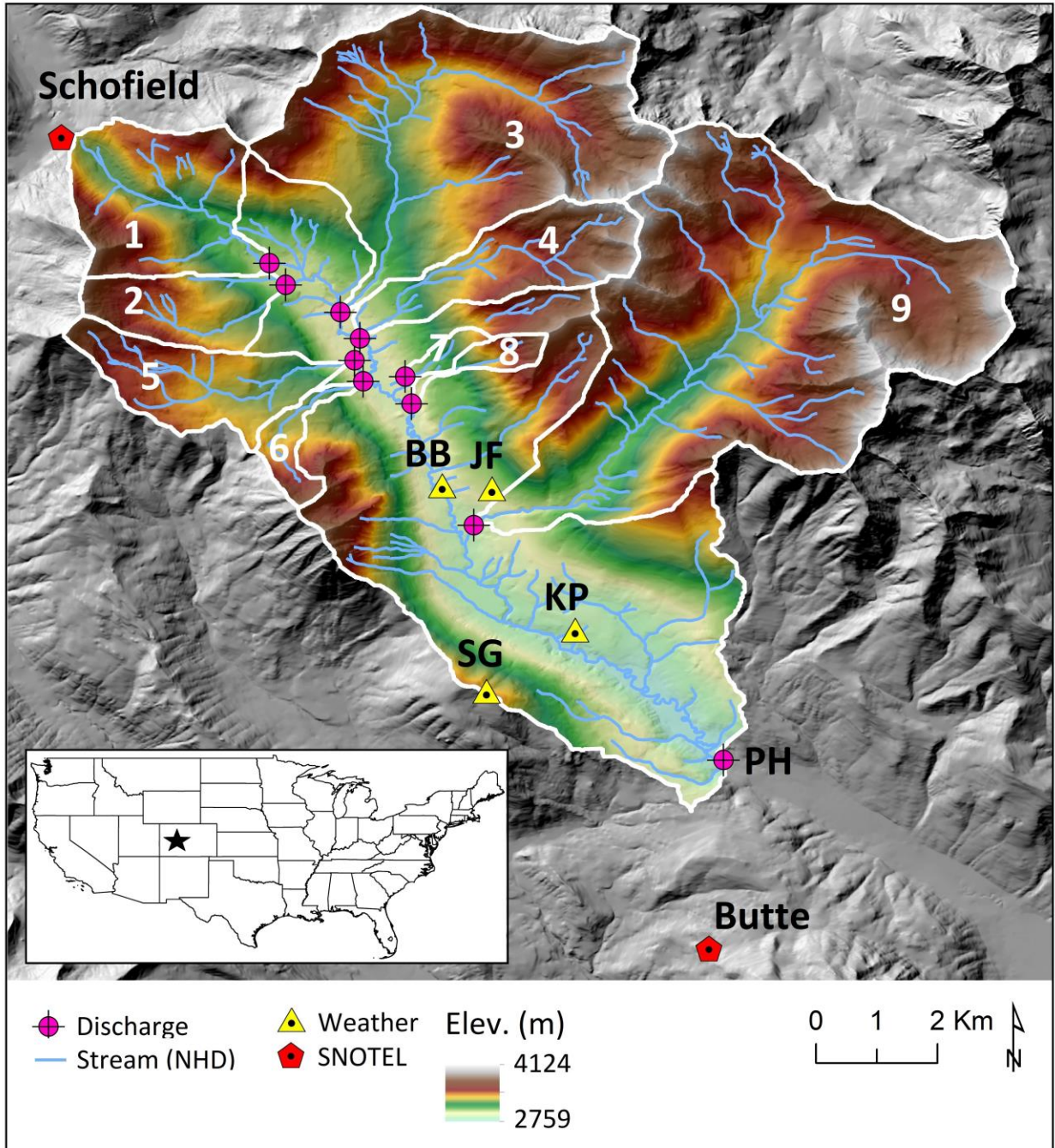
72 To capture these complex processes to better understand streamflow generation  
73 efficiency from NAM rains, we combine light detection and ranging (LiDAR) derived snow  
74 depths, precipitation and vegetation raster maps, an observation network of weather and stream  
75 discharge stations and a hydrologic numerical model of an alpine headwater basin of the  
76 Colorado River. Using this data-model framework, we pose the following questions over a multi-  
77 decadal, historical period: (i) How efficient are monsoon rains in generating streamflow and  
78 what are the principal controls on this efficiency? (ii) Can monsoon rains mitigate stream  
79 depletions from reduced snowfall and how important are they in promoting streamflow the  
80 following year?

## 81 **2 Site Description and Methods**

82 The study site is the East River, Colorado (ER, 85km<sup>2</sup>, Figure 1). Climate is continental  
83 subarctic. Snowmelt drives peak streamflow, typically occurring in early June and receding  
84 through the summer and fall. Observational networks related to snow and streamflow are  
85 described by others (Carroll *et al.*, 2018; Hubbard *et al.*, 2018; Carroll *et al.*, 2019) with station  
86 locations provided in Figure 1. ER elevations range from 2760 to 4065 m with pristine  
87 alpine/barren (26%), conifer (45%, spruce/fir), aspen (12%) and smaller coverages by shrubs,  
88 meadows and riparian conditions. Two Snow Telemetry (SNOTEL) stations reside in proximity  
89 of the ER (Figure 1, Schofield and Butte) with their period of record (1987-2019) capturing a  
90 wide range in snow accumulation and monsoon scenarios. Daily observations of solar radiation  
91 and snow depth are taken from four weather stations (Figure 1: SG, KP, JF and BB). Observed  
92 streamflow (years 2015-2019) are based on data from Carroll and Williams (2019) with subbasin  
93 characteristics provided in Table S1. In addition, observed daily streamflow at PH are regressed  
94 with the US Geological Survey (USGS) stream gauge (ID: 09112500) located 25 km  
95 downstream to approximate observed discharge over the entire simulation.

96 Hydrologic modeling builds upon previous work (Fang *et al.*, 2019; Carroll *et al.*, 2019)  
97 Daily water budgets are estimated with the USGS Precipitation-Modeling Runoff System  
98 (PRMS, Markstrom *et al.*, 2015). Water and energy are tracked within and between the  
99 atmosphere, plant, soil and groundwater and fluvial subcomponents of the watershed. The finite  
100 difference grid resolution is 100 m with elevations resampled from the USGS National Elevation  
101 Dataset. LANDFIRE (2015) is used to derive parameters of dominant cover type, summer and  
102 winter cover density, canopy interception characteristics for snow and rain and transmission  
103 coefficient for shortwave radiation. Climate forcing uses minimum and maximum daily  
104 temperature lapse rates defined by the two SNOTEL stations adjusted for aspect. Schofield  
105 snowfall is spatially distributed using LiDAR derived snow depth observations from the  
106 Airborne Snow Observatory (ASO, Painter *et al.*, 2016) flown 4 April 2016. Snow depths are  
107 converted to snow water equivalent (SWE) based on ground surveys and density modeling.  
108 Rainfall is spatially distributed using the monthly Parameter-elevation Relationships on

109



110

111 **Figure 1.** The East River and elevation with discharge, weather stations and sub-basins  
 112 identified. Streams from the National Hydrographic Dataset (NHD). Sub-basin ID: 1 = East  
 113 above Quigley (EAQ), 2 = Quigley, 3 = Rustlers, 4 = Bradley, 5 = Rock, 6 = Gothic, 7 =  
 114 Marmot, 8 = Avery, 9 = Copper, PH = Pumphouse. Inset shows East River location in the  
 115 continental United States.

116

117 Independent Slopes Model (PRISM, 800 m) 30-year (1981-2010) monthly averages (OSU, 2012)  
 118 (Figure S1). Simulated solar radiation is calibrated to match weather station observations. Model  
 119 verification of SWE accumulation and ablation relies on the 2018 and 2019 ASO maps and  
 120 weather station snow depth.

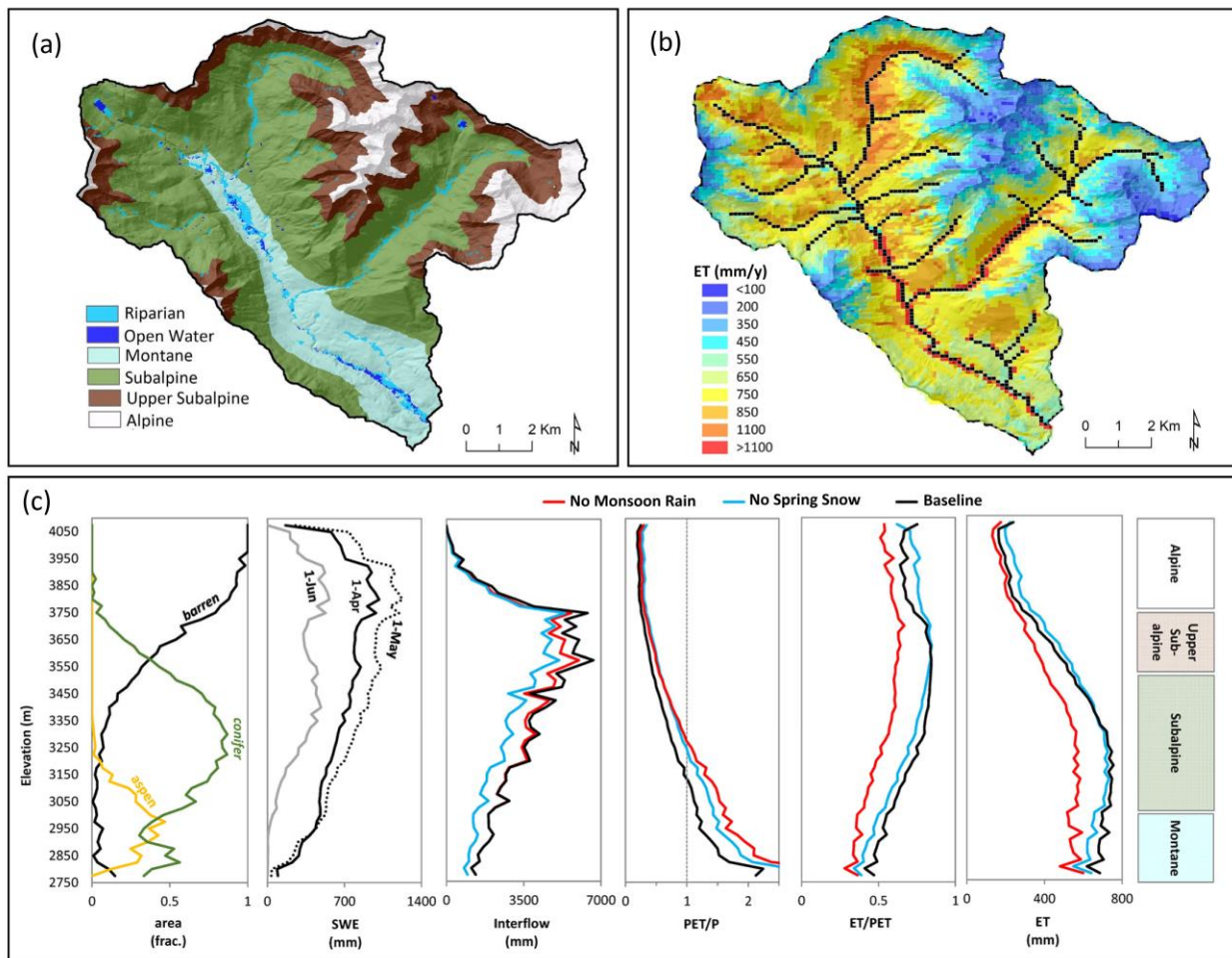
121 Maximum soil water storage is conceptualized as a field capacity threshold above which  
 122 water is partitioned to either shallow, lateral subsurface flow through the soil zone (interflow) or  
 123 allowed to percolate downward via gravity drainage into the deeper groundwater system. The  
 124 spatial distribution of soil storage is the product of rooting depth and available water content as a  
 125 function of soil type (NRCS, 1991). Parameters related to solar radiation, potential  
 126 evapotranspiration (PET), soil storage and groundwater transmissivity are adjusted at the  
 127 subbasin level to best match observed solar radiation and stream discharge. Model sensitivity to  
 128 seasonal precipitation is done by independently removing spring (April-May) or monsoon (July-  
 129 September) water inputs. Precipitation is removed for a single year and changes in water budget  
 130 components are compared to the historical (baseline) condition.

### 131 **3 Results**

132 Simulated daily solar radiation captures observed seasonal variability with a mean  
 133 monthly relative root mean squared error (rrmse) of 6.4% (Figure S2). Modeled SWE replicates  
 134 the spatial distribution of peak snow accumulation and late spring persistence during a dry year  
 135 2018, and peak accumulation in an extremely wet year 2019 (Figure S3); and mimics interannual  
 136 variability of snow depth at the four weather stations (Figure S4). Annual average streamflow at  
 137 all observed sites is modeled with rrmse of 2.4%. Daily flows (Figure S5) are well emulated for  
 138 most of the subbasins with Nash Sutcliffe Efficiency (NSE) for EAQ = 0.57, Quigley = 0.38,  
 139 Rustlers = 0.64, Rock = 0.66, and Copper = 0.67. PH has a NSE = 0.72 (log-flow NSE = 0.87)  
 140 for directly observed data and 0.71 (log-flow 0.73) using the USGS regression. Average annual  
 141 streamflow exiting the basin is  $2.16 \pm 0.48 \text{ m}^3/\text{s}$  ( $812 \pm 204 \text{ mm}/\text{y}$ ) with flow highest in June  
 142 ( $7.8 \pm 3.4 \text{ m}^3/\text{s}$ ) and lowest in February ( $0.42 \pm 0.19 \text{ m}^3/\text{s}$ ). Simulated precipitation is  $1413 \pm 233$   
 143  $\text{mm}/\text{y}$  with  $77 \pm 16\%$  falling as snow. Total annual ET for the baseline simulation is  $605 \pm 57$   
 144  $\text{mm}/\text{y}$ , or 43% total precipitation (P). ET components of sublimation, canopy evaporation and  
 145 soil ET are estimated at  $39 \pm 6 \text{ mm}/\text{y}$ ,  $138 \pm 19 \text{ mm}/\text{y}$  and  $428 \pm 41 \text{ mm}/\text{y}$ , respectively. Snow  
 146 dominates water inputs October-May. Rain dominates June-August when conditions are  
 147 typically water limited ( $\text{PET} > \text{P}$ ). Otherwise the basin is predominantly energy limited ( $\text{PET} < \text{P}$ )  
 148 (Figure S6). Monsoon precipitation is estimated  $251 \pm 94 \text{ mm}$ , or  $18 \pm 7\%$  annual water inputs with  
 149 interannual rain anomalies oscillating over a 7-10 year cycle with amplitude in anomalies  
 150 increasing 50% since 2013 (Figure S7). On average, spring precipitation in April and May  
 151 provide nearly equal inputs as the monsoon events ( $248 \pm 94 \text{ mm}$ ) though the interannual ratio is  
 152 highly variable.

153 Several water budget components are collapsed to a single dimension (elevation) in  
 154 Figure 2 for year 1998. Alpine conditions are defined above tree line ( $\geq 3750 \text{ m}$ ), while the  
 155 subalpine is defined as conifer coverage  $\geq 50\%$  by area (3525-3000 m). Montane occurs at the  
 156 lowest elevations where shrubs and aspen are dominant. Simulated SWE is largest in the alpine  
 157 and upper subalpine. For 1998, late season snow (post-April 1) increases across most of the  
 158 watershed by May 1, except at the lowest elevations where snowmelt exceeds any additional  
 159 snowfall. By June 1, declines in SWE occur across all elevations with all snow melted in the  
 160 montane. Interflow transports snowmelt downgradient with largest contributions into the upper  
 161 subalpine. Snowmelt driven interflow increases water availability for ET (ET/PET increases)

162 across all elevations with ET largest in the lower portions of the subalpine where conifer forests  
 163 are most abundant, canopy density is highest, and aridity is slightly water limited. At lower  
 164 elevations, water limiting conditions increase, lower snowpack and lower available interflow  
 165 reduce water availability for ET such that ET begins to decline as a consequence. The removal of  
 166 spring snow shifts water limited conditions to higher elevations compared to baseline. Interflow  
 167 decreases below the alpine zone. Total ET increases in the alpine and upper subalpine and  
 168 decreases in the lower portions of the subalpine and montane (refer to Figure S8 for changes in  
 169 the spatial distribution of ET). Removal of monsoon rain reduces interflow above the upper  
 170 subalpine but does increase aridity more in the lower subalpine and montane than removal of  
 171 spring snow. ET and ET/PET decreases across all elevations, with ET decreasing the most in the  
 172 lower subalpine.

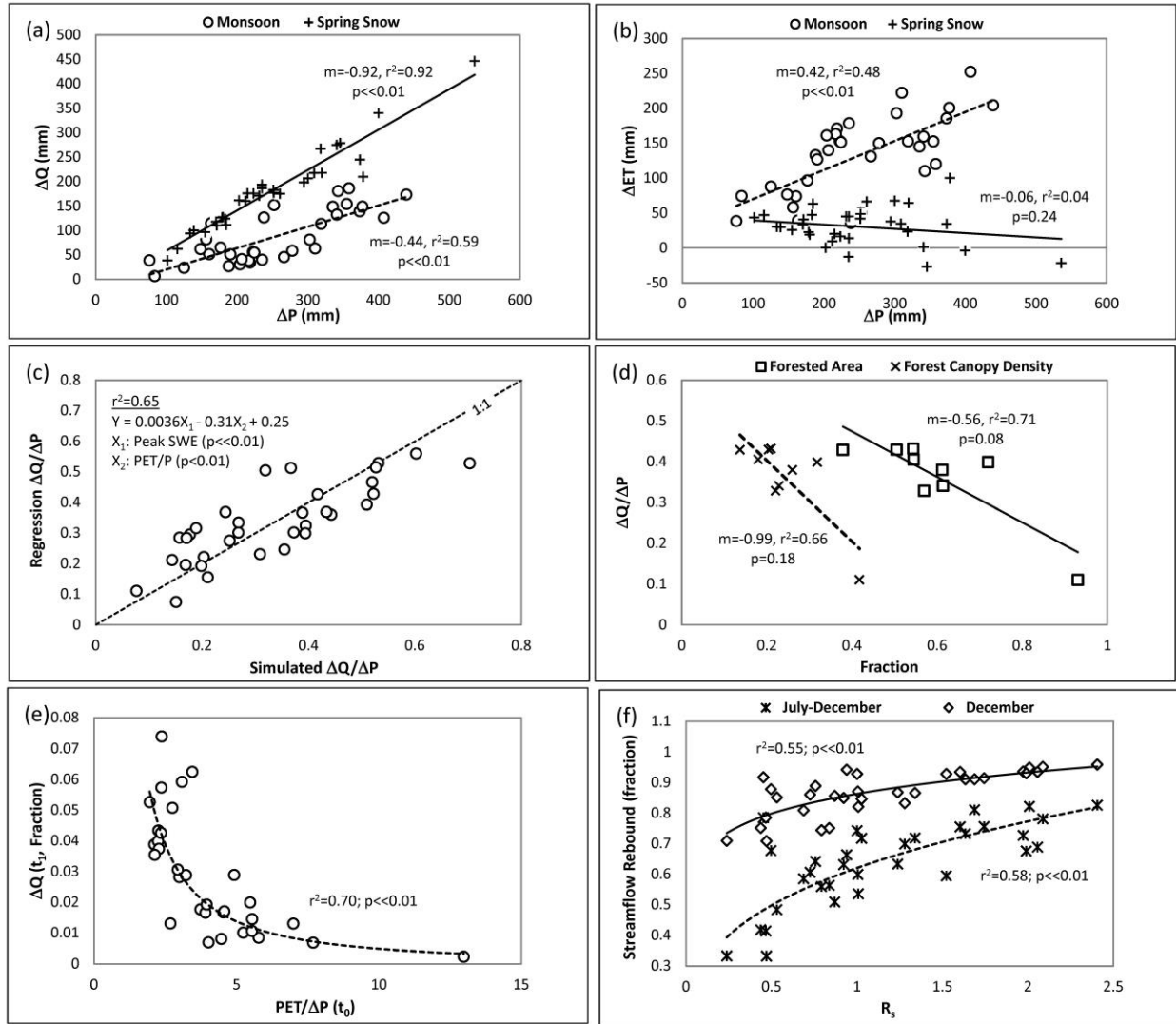


173

174 **Figure 2.** East River spatial trends in (a) ecosystems; and annual 1998 simulated (b) baseline  
 175 evapotranspiration (mm/y) as well as elevation dependence of (c) area-weighted vegetation,  
 176 snow water equivalent (SWE), interflow, aridity (PET/P), ET/PET and total ET. ‘No Monsoon  
 177 Rain’ removes precipitation July–September, No Spring Snow removes precipitation April- May.  
 178

179 Daily water budgets for four different years illustrate the range in basin response to  
180 reduced seasonal water inputs (Figure S9). The largest snow accumulation occurred in 1995,  
181 with low PET and average monsoon conditions. Year 1998 had median snow accumulation, with  
182 below average but equal inputs of spring snow and monsoon rain. Year 2012 had the lowest  
183 snowfall and warmest conditions in the historical simulation. There was little spring snow but  
184 near normal monsoon conditions. Year 2018 was also a low snow year with warm conditions but  
185 had a monsoon nearly two standard deviations below normal. Loss of spring snow, with  
186 emphasis on average and above average snow accumulation years, promotes higher soil moisture  
187 early in the spring and earlier onset of ET and runoff. These effects are largely due to increases  
188 in PET through simulated feedbacks with increased solar radiation and the influence of reduced  
189 snow-covered area on albedo and faster snowmelt (Figure S10). Shortly thereafter, lost  
190 snowpack reduces soil moisture in comparison to baseline, but soil moisture is largely  
191 replenished by monsoon rains, and ET only declines in dry years with declines amplified in years  
192 with weak monsoons. Streamflow, however, drops below baseline in all scenarios and becomes  
193 reliant on groundwater (versus interflow) earlier in the year. Removal of monsoon rain also  
194 increases solar radiation and PET and experiences soil moisture and streamflow deficits in  
195 comparison to baseline.

196 A schematic of seasonal water partitioning for spring snow and monsoon rain is given in  
197 Figure S11, while controls on the ability of seasonal water inputs to generate streamflow is  
198 explored with simple regression analysis using annual totals in Figure 3. On average, monsoon  
199 rain contributes  $10\pm 6\%$  to annual stream water. It is directly related to the amount of summer  
200 rain and is half as efficient at streamflow generation compared to spring snow for a given amount  
201 of water input. Monsoon rains support increases in basin scale ET ( $133\pm 56$  mm/y) and this is  
202 tightly controlled by the amount of rain. In contrast, increases in ET as a function of spring snow  
203 are much lower ( $31\pm 27$  mm/y) and this relationship declines with increases in contributing  
204 precipitation, albeit with a weak and insignificant trend ( $p=0.24$ ). Sixty-five percent of the  
205 simulated variance in monsoon rain efficiency (streamflow generation per unit precipitation  
206 input) is described by peak SWE ( $p\ll 0.01$ ) and PET ( $p<0.01$ ), while sub-basin efficiency is best  
207 described by the indirect relationship of the forest areal coverage ( $p=0.08$ ) and, to a lesser  
208 statistical degree, the canopy density ( $p=0.18$ ). The ability for monsoon rain to generate  
209 streamflow in the following year (lag 1) is modest ( $3\pm 2\%$  increase), especially in comparison to  
210 spring snowfall's influence ( $22\pm 17\%$ ). Increase in future flow due to monsoons rain is  
211 predominantly driven by the size of the monsoon ( $r^2 = 0.44$ ,  $p\ll 0.01$ ), but outlier years suggest  
212 the influence of monsoon rain increases when annual conditions are cool and PET is low  
213 ( $r^2=0.33$ ,  $p\ll 0.01$ ). A combined nonlinear function of total rain and PET describes 70% of  
214 simulated variability ( $p\ll 0.01$ ) and is able to explain sharp increases in subsequent year  
215 streamflow generation approaching 8%. Lastly, the ability of monsoon rain to replace late season  
216 streamflow deficiencies (July-Dec.) as a consequence of reduced spring snowfall is  $64\pm 13\%$ .  
217 Rebound in baseflow is directly related to the relative strength of monsoon inputs ( $R_s$ ) defined as  
218 the ratio of monsoon rain to spring snowfall reduction ( $p\ll 0.01$ ). Low  $R_s$  can only reduce  
219 deficiencies 33% while very large ratios ( $\sim 2.5$ ) allow an 83% recovery. By the end of December,  
220 monsoons replace streamflow deficiencies  $87\pm 7\%$  with no monsoon scenario obtaining 100%  
221 streamflow recovery.



222  
223

224 **Figure 3.** Annual water fluxes for 1987-2019. (a) Change in evapotranspiration ( $\Delta ET$ ) as a  
225 function of added precipitation ( $\Delta P$ ) from spring snow (April-May) or monsoon rain (July-Sept).  
226 (b) Change in streamflow ( $\Delta Q$ ) for added precipitation. (c) Predictive ability of peak snow water  
227 equivalent (SWE) and aridity (PET/P) to describe numerical model simulated monsoon  
228 streamflow generation efficiency ( $\Delta Q/\Delta P$ ). (d) Annual average efficiency for sub-basins in the  
229 East River as functions of forested area and forest canopy density. (e) Fractional increase in  
230 streamflow (lag 1,  $t_1$ ) as a power function of potential ET (PET) and amount of monsoon rain  
231 (lag 0,  $t_0$ ). (f) Fraction of streamflow rebound to baseline due to lost spring snow as a function of  
232 the ratio of monsoon precipitation to reduced spring snowfall ( $R_s$ ).

233 **4. Discussion**

234 The timing and intensity of the NAM is dominated by large-scale atmospheric processes  
235 (Zhu et al., 2005) but influences of localized, land surface conditions (e.g. soil moisture) could  
236 be important. Several studies have suggested there is an inverse relationship between winter  
237 snow accumulation and summer rainfall with decreased snow accumulation driving reduced soil

238 moisture such that less energy is needed to heat the land surface and this enhances the onset of  
239 rains (Gutzler, 2000; Lo & Clark, 2002; Zhu et al., 2005). In contrast, a positive soil moisture  
240 and rainfall feedback has been found by others (e.g. Vivoni, Tai and Gochis, 2009), while 470  
241 years of precipitation records reconstructed with tree ring data found the historical inverse  
242 relationship between summer and winter precipitation weak and unstable despite appearing  
243 stronger during the latter half of the 20<sup>th</sup> century (Griffin et al., 2013). It is acknowledged the  
244 hydrologic model used in this analysis does not account for large scale ocean-atmospheric  
245 coupling nor soil moisture–atmospheric feedbacks. However, the use of local climate data from  
246 SNOTEL sites distributed with LiDAR derived SWE in combination with data reanalysis  
247 products, indicates that ER summer rain anomalies do not track sea temperature indices such as  
248 the Southern Oscillation Index (Trenberth, 2020) or Pacific Decadal Oscillation (Mantua, 2020),  
249 nor show a clear correlation to soil moisture. However, summer rains in the ER do show a  
250 statistically significant and indirect correlation with cumulative snow water inputs and PET. This  
251 suggests years with low snow accumulation and warm conditions might produce more summer  
252 rain, though the multiple regression’s predictive power is low. Future work funded by the US  
253 Department of Energy’s Atmospheric Radiation Measurement research program will, in part,  
254 focus on capturing precipitation phase, amount and intensity in the ER as well as investigate  
255 regional flow of water into the continental interior during the summer monsoon  
256 (<https://www.arm.gov/news/facility/post/60749>). This work will help better constrain where,  
257 when and how summer rains enter the ER.

258 A clearer coupling occurs between soil moisture and stream water generation. Initial  
259 conditions of soil moisture can improve streamflow forecasts (Crow et al., 2018; Mahanama et  
260 al., 2012; Shahrban et al., 2018). However, the sensitivity of ET and streamflow to soil moisture  
261 is a function of where the system resides on the spectrum between energy and water availability  
262 (Budyko, 1974; Orth & Seneviratne, 2013). PET, or the maximum amount of water transferred  
263 back to the atmosphere from the land surface if water is not limiting, is a commonly used metric  
264 to define energy availability. It varies seasonally as a function of temperature, solar radiation,  
265 vapor pressure and wind speed (ASCE, 2005). Likewise, water availability varies in space and  
266 time. Water availability prior to monsoon onset is largely dictated by the previous season’s snow  
267 accumulation, redistribution and persistence (Hammond et al., 2018; Knowles et al., 2015) with  
268 these snow dynamics highly dependent on topography (Tennant et al., 2017) as well as  
269 vegetation type and structure (Bales et al., 2006; Broxton et al., 2015; Welch et al., 2016). Use  
270 of LiDAR snow observations accounts for where snow ends up, not necessarily where it fell. As  
271 such, the model implicitly accounts for snow redistribution by wind and avalanche as well as  
272 feedbacks between vegetation structure that may modify snow dynamics. Water availability also  
273 depends on lithologic and topographic characteristics that dictate water storage and holding  
274 capacity (Xiao et al., 2019) and the lateral redistribution of snowmelt via interflow (Carroll et al.,  
275 2019).

276 Research presented is largely inspired by exceptionally low NAM rain experienced in the  
277 ER 2018 and 2019 (z-score  $\sim -2$ ), and cited by regional water managers in Upper Colorado River  
278 for reducing late season flow to unprecedented levels (Sackett, 2018) and lowering streamflow  
279 forecasts the following year (Sackett, 2020). Because ET and streamflow are sensitive to energy  
280 and water availability and are highly co-dependent, it is important there is confidence that the  
281 hydrologic model captures these fluxes adequately for the baseline condition. The resultant,  
282 quasi-steady state water balance over multiple decades estimates annual ET equal to  $605 \pm 57$   
283 mm/y to balance incoming precipitation and outgoing streamflow. Streamflow is well

284 constrained by observations; and snowfall, or the bulk of water inputs, is also constrained by  
285 observations. Estimated basin average ET is larger than eddy covariance flux tower data located  
286 near PH ( $417 \pm 29$  mm/y) (Ryken et al., 2020), but is well aligned with Niwot Ridge eddy flux  
287 tower observations in a conifer (lodgepole) and aspen forest in Colorado (603 mm/y)  
288 ([ameriflux.lbl.gov](http://ameriflux.lbl.gov)). Simulated ER seasonal variance encapsulates Niwot observations, but the  
289 model estimates lower median rates in the winter and higher rates in June (Figure S12).  
290 Likewise, modeled summer rates exceed those presented by (Ryken et al., 2020). Simulated  
291 summer rates are largely biased by the areally extensive subalpine where both energy and water  
292 availability are high. In contrast, reduced summer rates are simulated in portions of the basin  
293 where either energy (alpine) or water limited (montane) conditions occur that more closely  
294 resemble the flux tower data. With respect to winter ET, modeled snow losses, or the sum of  
295 sublimation and snow-only canopy evaporation, is 0.37-0.66 mm/d, or  $17 \pm 9\%$  of snowfall.  
296 Sexstone et al., (2016) reports lower total snow loss rates from open canopy at 0.36 mm/d in a  
297 Colorado basin, but losses are 15-17% total snowfall to suggest our winter ET estimates are  
298 reasonable.

299 Model results indicate monsoon rains generate  $10 \pm 6\%$  the annual streamflow total with  
300 these contributions helping to sustain late season baseflow. Results fall in the reported range of  
301 streamflow generated from rain across the western US at 30% (Li et al., 2017), and 1-2%  
302 (Julander & Clayton, 2018), with the lower limit occurring in more arid climates than the ER.  
303 Years with large snow accumulation and low atmospheric water demand directly describe the  
304 efficiency of monsoon rain to generate streamflow. Under these conditions, soil moisture holding  
305 capacity is exceeded for lower amounts of water input to allow more interflow, with a portion of  
306 interflow reaching stream channels. While snowmelt generated interflow occurs across all  
307 elevations, interflow from monsoon rain is largely constrained above treeline where soils are  
308 thin, and PET is low. Lower in the landscape, and along southern aspects, aridity (PET/P) is  
309 higher and is simulated more sensitive in solar radiation as a function of altering seasonal  
310 precipitation and inferred cloud cover. Sensitivity of PET to solar radiation in warmer conditions  
311 has been shown with similar, empirically-based methods (e.g. Priestley-Taylor) (Guo et al.,  
312 2017) to that used in PRMS (Jensen et al., 1969). These lower elevations, with emphasis in the  
313 subalpine forests, effectively eliminates streamflow response to monsoon rain through resulting  
314 increases in ET. In short, monsoon water inputs have a relatively small effect on streamflow  
315 through moderating effects of ET. Additionally, the ability of rain to generate streamflow is  
316 expected to decline in a future with less snow and warmer temperatures. In contrast, snowfall has  
317 a more complex relationship to ET in space and time driven by albedo-snowmelt feedbacks that  
318 substantively shift timing of melt and subsequent runoff (Barnett et al., 2005), but show  
319 relatively small net changes in ET compared to monsoon rains. The lower efficiency of ET to  
320 snowmelt is due to the timing of inputs prior to peak consumptive demand. This is supported by  
321 Berkelhammer et al. (2017) who found gross primary production (via satellite retrievals of solar-  
322 induced variability) in the intermountain west twice as sensitive to variations in rain compared to  
323 snow.

324 Despite differences in streamflow generation efficiencies, monsoon rain does help  
325 rebound baseflow deficiencies caused by a reduction snow accumulation. This ability is highly  
326 dependent on the relative strength of the monsoon, and no historical monsoon season can fully  
327 replenish streamflow deficits caused by hypothetical lost spring snowpack. This indicates that  
328 soil moisture dictated by snowmelt has long lasting effects on streamflow that cannot be fully  
329 reversed with summer rain. Likewise, soil moisture memory from summer rains is hypothesized

330 to also impose on future streamflow. McNamara et al. (2005) finds remnant dry soils in the fall  
331 remain dry once snowfall commences, and these dry soils require more meltwater than wet soils  
332 to produce lateral movement of water in the spring. Thereby decreasing streamflow. Our model  
333 predicts monsoon memory on future streamflow, but this the effect is modest with average  
334 annual change to future flow only to  $3\pm 2\%$ . Memory is controlled by the size of the monsoon  
335 and atmospheric water demand and shows no correlation to late season soil moisture. This lack  
336 of simulated response may be due to the simplistic soil conceptualization in the hydrologic  
337 model; or it may be thin soils in headwater basins are rewetted quickly by low quantities of  
338 snowmelt in comparison to the large quantities of snow available. These relationships may  
339 change as one moves down gradient in the Colorado River to warmer and drier climates, or if  
340 snow droughts continue to increase throughout the region to reduce snow accumulation in the  
341 ER. However, this requires a more detailed process-based investigation.

## 342 **5 Conclusions**

343 Summer rains are a critical water input to the ER with the amplitude of monsoon  
344 anomalies growing in the basin since 2013 and inspiring questions related to the efficiency of  
345 monsoon rains to generate streamflow. This is particularly important in the Colorado River Basin  
346 where snowpack is decreasing, and it is unknown if summer rains can buffer some of these  
347 losses. We find through a data-modeling framework that the efficiency of seasonal precipitation  
348 to produce streamflow is dictated by the timing of water input with respect to energy and water  
349 availability. Summer rains occur when PET is high and soil moisture is waning during the pre-  
350 monsoon drought. Subsequently, the bulk of rain serves to moisten very dry soils and does not  
351 generate interflow. Instead, water is quickly consumed by vegetation, with largest increases in  
352 ET occurring in the lower subalpine dominated by aspen and conifer forests. As a result,  
353 streamflow contributions from rain are half those generated by spring snowfall which occur  
354 when PET is low and soils moisture is higher. Most of the rain-generated streamflow occurs at  
355 higher elevations in the watershed where soil storage, forest cover and aridity are low. Summer  
356 rain does rebound late summer streamflow from simulated reductions in snowpack as a function  
357 of monsoon strength but is unable to fully replace streamflow from lost snow accumulation even  
358 for the largest historical monsoon event. Results do show memory of monsoon rains propagate  
359 into the following year through altered baseflow, but do not indicate memory as a function of fall  
360 soil moisture condition. Interannual variability in monsoon efficiency to generate streamflow  
361 declines when snowpack is low and aridity is high. This underscores the likelihood that the  
362 ability of monsoon rain to generate streamflow will decline in a warmer future with increased  
363 snow drought.

## 364 **Acknowledgments and Data**

365 Model characterization, validation and additional results are provided in the Supporting  
366 Information. Model input and output files are available to the public on the US Department of  
367 Energy (DOE) Environmental Systems Science Data Infrastructure for Virtual Ecosystem (ESS-  
368 DIVE DOI placeholder). Work is supported by the US DOE Office of Science under contract  
369 DE-AC02-05CH11231 as part of Lawrence Berkeley National Laboratory Watershed Function  
370 Science Focus Area. Additional support from Boise State University DOE contract DE-  
371 SC0019222.

372 **References**

- 373 ASCE. (2005). *The ASCE standardized reference evapotranspiration equation*, Technical  
 374 Committee Report to the Environmental and Water Resources Institute of the American  
 375 Society of Civil Engineers from the Task Committee on Standardization of Reference  
 376 Evapotranspiration. [https://www.mesonet.org/images/site/  
 377 ASCEEvapotranspiration\\_Formula.pdf](https://www.mesonet.org/images/site/ASCEEvapotranspiration_Formula.pdf)
- 378 Bales, R. C., Molotch, N. P., Painter, T. H., Dettinger, M. D., Rice, R., & Dozier, J. (2006).  
 379 Mountain hydrology of the western United States. *Water Resources Research*, 42(8), 1–13.  
 380 <https://doi.org/10.1029/2005WR004387>
- 381 Bales, R., Molotch, N., Painter, T., Dettinger, M., Rice, R., & Dozier, J. (2006). Mountain  
 382 hydrology of the Western United States. *Water Resources Research*, 42, 1208.  
 383 <https://doi.org/doi:10.1029/2005WR004387>
- 384 Barnett, T. P., Adam, J. C., & Lettenmaier, D. P. (2005). Potential impacts of a warming climate  
 385 on water availability in snow-dominated regions. *Nature*, 438, 303–309.  
 386 <https://doi.org/http://dx.doi.org/10.1038/nature04141>.
- 387 Berkelhammer, M., Stefanescu, I. C., Joiner, J., & Anderson, L. (2017). High sensitivity of gross  
 388 primary production in the Rocky Mountains to summer rain. *Geophysical Research Letters*,  
 389 44(8), 3643–3652. <https://doi.org/10.1002/2016GL072495>
- 390 Broxton, P. D., Harpold, A. A., Biederman, J. A., Troch, P. A., Molotch, N. P., & Brooks, P. D.  
 391 (2015). Quantifying the effects of vegetation structure on snow accumulation and ablation  
 392 in mixed-conifer forests. *Ecohydrology*, 8(6), 1073–1094. <https://doi.org/10.1002/eco.1565>
- 393 Budyko, M. I. (1974). *Climate and Life*. Elsevier.
- 394 Carroll, R.W.H., & Williams, K. H. (2019). Discharge data collected within the East River for  
 395 the Lawrence Berkeley National Laboratory Watershed Function Science Focus Area  
 396 (Water years 2015-2018). *ESS-DIVE*.  
 397 <https://doi.org/http://dx.doi.org/10.21952/WTR/1465929>
- 398 Carroll, Rosemary W. H., Deems, J. S., Niswonger, R., Schumer, R., & Williams, K. H. (2019).  
 399 The Importance of Interflow to Groundwater Recharge in a Snowmelt-Dominated  
 400 Headwater Basin. *Geophysical Research Letters*, 46(11), 5899–5908.  
 401 <https://doi.org/10.1029/2019GL082447>
- 402 Carroll, Rosemary W.H., Bearup, L. A., Brown, W., Dong, W., Bill, M., & Williams, K. H.  
 403 (2018). Factors controlling seasonal groundwater and solute flux from snow-dominated  
 404 basins. *Hydrological Processes*, 32(14), 2187–2202. <https://doi.org/10.1002/hyp.13151>
- 405 Carroll, Rosemary W.H., Deems, J. S., Niswonger, R., Schumer, R., & Williams, K. H. (2019).  
 406 The Importance of Interflow to Groundwater Recharge in a Snowmelt-Dominated  
 407 Headwater Basin. *Geophysical Research Letters*, 46(11), 5899–5908.  
 408 <https://doi.org/10.1029/2019GL082447>
- 409 Crow, W. T., Chen, F., Reichle, R. H., Xia, Y., & Liu, Q. (2018). Exploiting Soil Moisture,  
 410 Precipitation, and Streamflow Observations to Evaluate Soil Moisture/Runoff Coupling in  
 411 Land Surface Models. *Geophysical Research Letters*, 45(10), 4869–4878.  
 412 <https://doi.org/10.1029/2018GL077193>

- 413 Deems, J. S., Fassnacht, S. R., & Elder, K. J. (2006). Fractal distribution of snow depth from  
414 LiDAR data. *Journal of Hydrometeorology*, 7, 285–297.
- 415 Fang, Z., Carroll, R. W. H., Schumer, R., Harman, C., Wilusz, D., & Williams, K. H. (2019).  
416 Streamflow partitioning and transit time distribution in snow-dominated basins as a function  
417 of climate. *Journal of Hydrology*, 570(December 2018), 726–738.  
418 <https://doi.org/10.1016/j.jhydrol.2019.01.029>
- 419 Griffin, D., Woodhouse, C. A., Meko, D. M., Stahle, D. W., Faulstich, H. L., Carrillo, C.,  
420 Touchan, R., Castro, C. L., & Leavitt, S. W. (2013). North American monsoon precipitation  
421 reconstructed from tree-ring latewood. *Geophysical Research Letters*, 40(5), 954–958.  
422 <https://doi.org/10.1002/grl.50184>
- 423 Guo, D., Westra, S., & Maier, H. R. (2017). Sensitivity of potential evapotranspiration to  
424 changes in climate variables for different Australian climatic zones. *Hydrology and Earth  
425 System Sciences*, 21(4), 2107–2126. <https://doi.org/10.5194/hess-21-2107-2017>
- 426 Gutzler, D. S. (2000). Covariability of spring snowpack and summer rainfall across the  
427 Southwest United States. *Journal of Climate*, 13(22), 4018–4027.  
428 [https://doi.org/10.1175/1520-0442\(2000\)013<4018:COSSAS>2.0.CO;2](https://doi.org/10.1175/1520-0442(2000)013<4018:COSSAS>2.0.CO;2)
- 429 Hall, A. (2004). The role of surface albedo feedback in climate. *Journal of Climate*, 17(7), 1550–  
430 1568. [https://doi.org/10.1175/1520-0442\(2004\)017<1550:TROSAF>2.0.CO;2](https://doi.org/10.1175/1520-0442(2004)017<1550:TROSAF>2.0.CO;2)
- 431 Hammond, J. C., Saavedra, F. A., & Kampf, S. K. (2018). How does snow persistence relate to  
432 annual streamflow in mountain watersheds of the western U.S. with wet maritime and dry  
433 continental climates? *Water Resources Research*, 54(4), 2605–2623.  
434 <https://doi.org/doi:10.1002/2017WR021899>
- 435 Harpold, A., Brooks, P., Rajagopal, S., Heidbuchel, I., Jardine, A., & Stielstra, C. (2012).  
436 Changes in snowpack accumulation and ablation in the intermountain west. *Water  
437 Resources Research*, 48(11). <https://doi.org/10.1029/2012WR011949>
- 438 Hock, R., Rasul, G., Adler, C., Cáceres, B., Gruber, S., Hirabayashi, Y., Jackson, M., Kääh, A.,  
439 Kang, S., Kutuzov, S., Milner, A., Molau, U., Morin, S., Orlove, B., & Steltzer, H. I.  
440 (2019). Chapter 2: High Mountain Areas. IPCC Special Report on the Ocean and  
441 Cryosphere in a Changing Climate. *IPCC Special Report on the Ocean and Cryosphere in a  
442 Changing Climate*, 131–202.
- 443 Hubbard, S. S., Williams, K. H., Agarwal, D., Banfield, J., Beller, H., Bouskill, N., Brodie, E.,  
444 Carroll, R., Dafflon, B., Dwivedi, D., Falco, N., Faybishenko, B., Maxwell, R., Nico, P.,  
445 Steefel, C., Steltzer, H., Tokunaga, T., Tran, P. A., Wainwright, H., & Varadharajan, C.  
446 (2018). The East River, Colorado, watershed: A mountainous community testbed for  
447 improving predictive understanding of multiscale hydrological–biogeochemical dynamics.  
448 *Vadose Zone Journal*, 17(1). <https://doi.org/10.2136/vzj2018.03.0061>
- 449 Huning, L. S., & AghaKouchak, A. (2020). Global snow drought hot spots and characteristics.  
450 *Proceedings of the National Academy of Sciences*, 201915921.  
451 <https://doi.org/10.1073/pnas.1915921117>
- 452 Jacobs, J. (2011). Sustainability of Water Resources in the Colorado River Basin. *The Bridge:  
453 Linking Engineering and Society*, 41((winter)), 6–12.

- 454 Jensen, M. E., Rob, D. C. N., & Franzoy, C. E. (1969). Scheduling irrigations using climate-  
455 crop-soil data. *National Conference on Water Resources Engineering of the American*  
456 *Society of Civil Engineers*, 20 p.
- 457 Julander, R. P., & Clayton, J. A. (2018). Determining the proportion of streamflow that is  
458 generated by cold season processes versus summer rainfall in Utah, USA. *Journal of*  
459 *Hydrology: Regional Studies*, 17(December 2017), 36–46.  
460 <https://doi.org/10.1016/j.ejrh.2018.04.005>
- 461 Knowles, J. F., Harpold, A. A., Cowie, R., Zeff, M., Barnard, H. R., Burns, S. P., Blanken, P.  
462 D., Morse, J. F., & Williams, M. W. (2015). The relative contributions of alpine and  
463 subalpine ecosystems to the water balance of a mountainous, headwater catchment.  
464 *Hydrological Processes*, 29(22), 4794–4808. <https://doi.org/10.1002/hyp.10526>
- 465 LANDFIRE. (2015). *Existing vegetation type and cover layers*. U.S. Department of the Interior,  
466 Geological Survey. <http://landfire.cr.usgs.gov/viewer/>(accessed May 2017)
- 467 Li, D., Wrzesien, M. L., Durand, M., Adam, J., & Lettenmaier, D. P. (2017). How much runoff  
468 originates as snow in the western United States, and how will that change in the future?  
469 *Geophysical Research Letters*, 6163–6172. <https://doi.org/10.1002/2017GL073551>
- 470 Lo, F., & Clark, M. P. (2002). Relationships between spring snow mass and summer  
471 precipitation in the Southwestern United States associated with the North American  
472 monsoon system. *Journal of Climate*, 15(11), 1378–1385. [https://doi.org/10.1175/1520-0442\(2002\)015<1378:RBSSMA>2.0.CO;2](https://doi.org/10.1175/1520-0442(2002)015<1378:RBSSMA>2.0.CO;2)
- 474 Ma, J., Zhang, T., Guan, X., Hu, X., Duan, A., & Liu, J. (2019). The dominant role of snow/ice  
475 Albedo feedback strengthened by black carbon in the enhanced warming over the  
476 Himalayas. *Journal of Climate*, 32(18), 5883–5899. <https://doi.org/10.1175/JCLI-D-18-0720.1>
- 478 Mahanama, S., Livneh, B., Koster, R., Lettenmaier, D., & Reichle, R. (2012). Soil moisture,  
479 snow, and seasonal streamflow forecasts in the United States. *Journal of*  
480 *Hydrometeorology*, 13(1), 189–203. <https://doi.org/10.1175/JHM-D-11-046.1>
- 481 Mantua, N. (2020). *Pacific Decadal Oscillation (PDO)*.  
482 <http://research.jisao.washington.edu/pdo/PDO.latest>
- 483 Markstrom, S. L., Regan, R. S., Hay, L. E., Viger, R. J., Webb, R. M. T., Payn, R. A., &  
484 LaFontaine, J. H. (2015). PRMS-IV, the precipitation-runoff modeling system, version 4.  
485 *U.S. Geological Survey Techniques and Methods, Book 6, Chap. B7*, 158.  
486 <https://doi.org/http://dx.doi.org/10.3133/tm6B7>
- 487 McNamara, J. P., Chandler, D., Seyfried, M., & Achet, S. (2005). Soil moisture states, lateral  
488 flow, and streamflow generation in a semi-arid, snowmelt-driven catchment. *Hydrological*  
489 *Processes*, 19(20), 4023–4038. <https://doi.org/10.1002/hyp.5869>
- 490 Milly, P. C. D., & Dunne, K. A. (2020). *Colorado River flow dwindles as warming-driven loss of*  
491 *reflective snow energizes evaporation*. 9187(February), 1–9.
- 492 Mote, P. W., Li, S., Lettenmaier, D. P., Xiao, M., & Engel, R. (2018). Dramatic declines in  
493 snowpack in the western US. *Npj Climate and Atmospheric Science*, 1(1), 2.  
494 <https://doi.org/10.1038/s41612-018-0012-1>

- 495 NRCS. (1991). *Web Soil Survey*. United States Department of Agriculture.  
496 <http://websoilsurvey.nrcs.usda.gov/> accessed March 2016
- 497 Orth, R., & Seneviratne, S. I. (2013). Propagation of soil moisture memory to streamflow and  
498 evapotranspiration in Europe. *Hydrology and Earth System Sciences*, 17(10), 3895–3911.  
499 <https://doi.org/10.5194/hess-17-3895-2013>
- 500 OSU. (2012). *PRISM Climate Group*. <http://prism.oregonstate.edu>
- 501 Painter, T. H., Berisford, D. F., Boardman, J. W., Bormann, K. J., Deems, J. S., Gehrke, F.,  
502 Hedrick, A., Joyce, M., Laidlaw, R., Marks, D., Mattmann, C., McGurk, B., Ramirez, P.,  
503 Richardson, M., Skiles, S. M. K., Seidel, F. C., & Winstral, A. (2016). The Airborne Snow  
504 Observatory: Fusion of scanning lidar, imaging spectrometer, and physically-based  
505 modeling for mapping snow water equivalent and snow albedo. *Remote Sensing of*  
506 *Environment*, 184, 139–152. <https://doi.org/10.1016/j.rse.2016.06.018>
- 507 Ryken, A. E. C., Gochis, D., & Maxwell, R. (2020). Unraveling groundwater contributions to  
508 evapotranspiration in a mountain headwaters: Using eddy covariance to constrain water and  
509 energy fluxes in the East River Watershed. *Authorea*.  
510 <https://doi.org/10.22541/au.159559979.93668749>
- 511 Sackett, H. (2018, October 2). Colorado's 2018 water year closes out as one of the driest on  
512 record. *Aspen Times*. [https://www.aspentimes.com/news/local/colorados-2018-water-year-](https://www.aspentimes.com/news/local/colorados-2018-water-year-closes-one-of-driest-on-record/)  
513 [closes-one-of-driest-on-record/](https://www.aspentimes.com/news/local/colorados-2018-water-year-closes-one-of-driest-on-record/)
- 514 Sackett, H. (2020, April 13). Streamflow forecast down for Roaring Fork despite above-normal  
515 snowpack. *Aspen Times*. [https://www.aspentimes.com/news/streamflow-forecast-down-for-](https://www.aspentimes.com/news/streamflow-forecast-down-for-roaring-fork-despite-above-normal-snowpack/)  
516 [roaring-fork-despite-above-normal-snowpack/](https://www.aspentimes.com/news/streamflow-forecast-down-for-roaring-fork-despite-above-normal-snowpack/)
- 517 Sexstone, G. A., Clow, D. W., Stannard, D. I., & Fassnacht, S. R. (2016). Comparison of  
518 methods for quantifying surface sublimation over seasonally snow-covered terrain.  
519 *Hydrological Processes*, 30(19), 3373–3389. <https://doi.org/10.1002/hyp.10864>
- 520 Shahrban, M., Walker, J. P., Wang, Q. J., & Robertson, D. E. (2018). On the importance of soil  
521 moisture in calibration of rainfall–runoff models: two case studies. *Hydrological Sciences*  
522 *Journal*, 63(9), 1292–1312. <https://doi.org/10.1080/02626667.2018.1487560>
- 523 Sheppard, P. R., Comrie, A. C., Packin, G. D., Angersbach, K., & Hughes, M. K. (2002). The  
524 climate of the US Southwest. *Climate Research*, 21(3), 219–238.  
525 <https://doi.org/10.3354/cr021219>
- 526 Tennant, C. (2016). *Laser vision : LiDAR illuminates the influence of climate , topography , and*  
527 *vegetation on seasonal snowpack*.
- 528 Tennant, C. J., Harpold, A., Lohse, K. A., Godsey, S. E., Crosby, B. T., Larsen, L. G., Brooks, P.  
529 D., Van Kirk, R. W., & Glen, N. F. (2017). Regional sensitivities of seasonal snowpack to  
530 elevation, aspect, and vegetation cover in western North America. *Water Resources*  
531 *Research*. <https://doi.org/10.1002/2016 WR019374>
- 532 Trenberth, K. (2020). *The Climate Data Guide: Southern Oscillation Indices: Signal, Noise and*  
533 *Tahiti/Darwin SLP (SOI)*. [https://climatedataguide.ucar.edu/climate-data/southern-](https://climatedataguide.ucar.edu/climate-data/southern-oscillation-indices-signal-noise-and-tahitidarwin-slp-soi)  
534 [oscillation-indices-signal-noise-and-tahitidarwin-slp-soi](https://climatedataguide.ucar.edu/climate-data/southern-oscillation-indices-signal-noise-and-tahitidarwin-slp-soi).
- 535 Vano, J. A., Das, T., & Lettenmaier, D. P. (2012). Hydrologic Sensitivities of Colorado River

- 536           Runoff to Changes in Precipitation and Temperature. *Journal of Hydrometeorology*, 13(3),  
537           932–949. <https://doi.org/10.1175/JHM-D-11-069.1>
- 538   Vivoni, E. R., Tai, K., & Gochis, D. J. (2009). Effects of initial soil moisture on rainfall  
539           generation and subsequent hydrologic response during the North American monsoon.  
540           *Journal of Hydrometeorology*, 10(3), 644–664. <https://doi.org/10.1175/2008JHM1069.1>
- 541   Welch, C. M., Stoy, P. C., Rains, F. A., Johnson, A. V., & Mcglynn, B. L. (2016). The impacts  
542           of mountain pine beetle disturbance on the energy balance of snow during the melt period.  
543           *Hydrological Processes*, 30(4), 588–602. <https://doi.org/10.1002/hyp.10638>
- 544   Xiao, D., Shi, Y., Brantley, S. L., Forsythe, B., DiBiase, R., Davis, K., & Li, L. (2019).  
545           Streamflow Generation From Catchments of Contrasting Lithologies: The Role of Soil  
546           Properties, Topography, and Catchment Size. *Water Resources Research*, 55(11), 9234–  
547           9257. <https://doi.org/10.1029/2018WR023736>
- 548   Zhu, C., Lettenmaier, D. P., & Cavazos, T. (2005). Role of antecedent land surface conditions of  
549           North American monsoon rainfall variability. *Journal of Climate*, 18(16), 3104–3121.  
550           <https://doi.org/10.1175/JCLI3387.1>
- 551